

Frank's constant in the hexatic phase

P. Keim, G. Maret*, and H.H. von Grünberg
 Universität Graz, 8010 Graz, Austria
 *Universität Konstanz, 78457 Konstanz, Germany
 (Dated: April 15, 2024)

Using video-microscopy data of a two-dimensional colloidal system the bond-order correlation function G_6 is calculated and used to determine the temperature-dependence of both the orientational correlation length ξ_6 in the isotropic liquid phase and the Frank constant F_A in the hexatic phase. F_A takes the value 72π at the hexatic \rightarrow isotropic liquid phase transition and diverges at the hexatic \rightarrow crystal transition as predicted by the KTHNY-theory. This is a quantitative test of the mechanism of breaking the orientational symmetry by disclination unbinding.

PACS numbers: 64.70.Dv, 68.35.Rh, 82.70.Dd

The theory of melting in two dimensions (2d) developed by Kosterlitz, Thouless, Halperin, Nelson and Young (KTHNY-theory) suggests a two-stage melting from the crystalline phase to the isotropic liquid. The first transition at temperature T_m is driven by the dissociation of thermally activated dislocation pairs into isolated dislocations breaking the translational symmetry [1, 2]. The liquid phase directly above T_m still exhibits orientational symmetry and is called the hexatic phase. It may be viewed as an anisotropic liquid with a six-fold director [3, 4] which is characterized by a finite value of Frank's constant F_A , the elastic modulus quantifying the orientational stiffness. At the second transition at $T_i > T_m$, the dissociation of some of the dislocations into free disclinations destroys the orientational symmetry. Now, the liquid shows ordinary short-range rotational and positional order as it is characteristic of an isotropic liquid.

Following an argument given in [1, 4], T_m and T_i can be estimated using the defect interaction Hamiltonian H_d between a pair of disclinations ($d = \text{disc}$) and a pair of dislocations ($d = \text{disl}$) which for both defect pairs and at large distances goes like $H_d \sim c_d \log r$ with the dimensionless strength parameter c_d depending on the defect type. Defect dissociation is completed at a temperature where the thermally averaged pair distance $\langle r_d^2 \rangle$ diverges. Evaluating this expression for H_d one generally finds divergence if $c_d = 4$. The unbinding condition $c_d = 4$ translates into $\lim_{T \rightarrow T_m} K(T) a_0^2 = 16$ for dislocation pairs ($\epsilon = 1 = k_B T$, a_0 is lattice spacing) and into $\lim_{T \rightarrow T_i} F_A(T) = 72\pi$ for disclination pairs, where K is the Young's modulus of the crystal. Connecting thus the defect pair unbinding condition to the two transition temperatures T_i and T_m , two expressions are obtained that summarize the microscopic explanation of the KTHNY theory for two-stage melting.

In this Letter we study the temperature-dependence of Frank's constant of a 2D system in the hexatic phase. We first determine the hexatic \rightarrow isotropic liquid transition temperature T_i and then check if Frank's constant takes the value 72π at T_i , thus testing the KTHNY theory

and its prediction that disclination unbinding occurs at T_i . In addition, we analyze the divergence behavior of the orientational correlation length at T_i and of Frank's constant at T_m .

Different theoretical approaches invoking grain boundary induced melting [5, 6] or condensation of geometrical defects [7, 8] suggest one first order transition. However some simulations for Lennard-Jones systems indicate the hexatic phase to be metastable [9, 10]. The transition in hard-core systems seem to be first-order [12] probably due to finite-size effects [11]. Simulations with long-range dipole-dipole interaction clearly show second order behavior [13]. Experimental evidence for the hexatic phase has been demonstrated for colloidal systems [14, 15, 16, 17, 18, 19], in block copolymer films [20, 21], as well as for magnetic bubble arrays and microscopic granular or atomic systems [22, 23, 24, 25, 26]. Still the order of the transitions is seen to be inconsistent. The observation of a phase equilibrium isotropic/hexatic [17, 21] and hexatic/crystalline [17] indicates two first order transitions. In our system we find two continuous transitions.

The experimental setup is essentially the same as in [27]. Spherical and super-paramagnetic colloids (diameter $d = 4.5 \mu\text{m}$) are confined by gravity to a water/air interface formed by a water drop suspended by surface tension in a top sealed cylindrical hole of a glass plate. The field of view has a size of $835 \times 620 \mu\text{m}^2$ containing typically up to 3×10^6 particles (out of 3×10^8 of the whole sample). A magnetic field H is applied perpendicular to the air/water interface inducing in each particle a magnetic moment $M = \chi H$. This leads to a repulsive dipole-dipole pair-interaction with the dimensionless interaction strength given by $\epsilon = (\chi_0 = 4) (\chi H)^2 (\rho)^{-3} = 2$. Here χ is the susceptibility per colloid while ρ is the 2d particle density and the average particle distance is $a = 1/\rho$. The interaction strength can be externally controlled by means of the magnetic field H ; it can be interpreted as an inverse temperature and is the only parameter controlling the phase behavior of the system. For each (x, y) the coordinates of the colloids are recorded

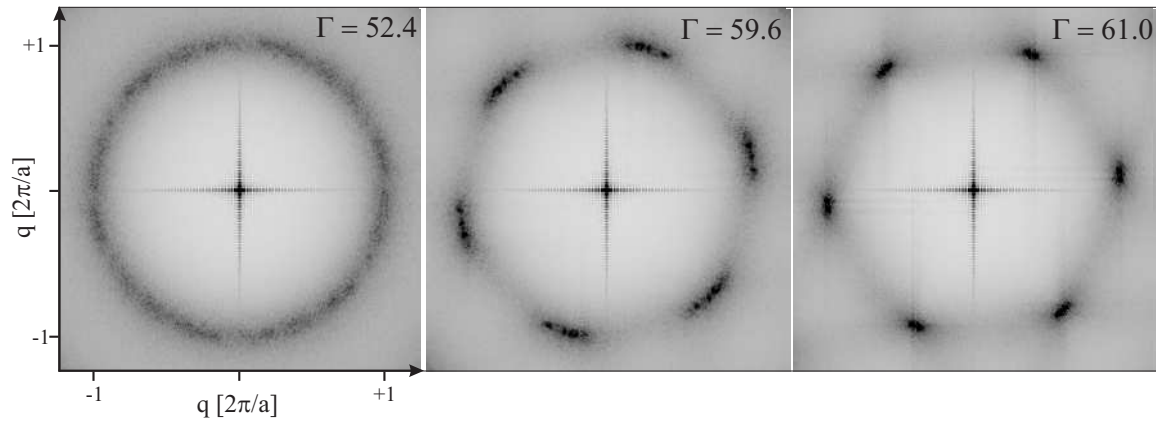


FIG. 1: Structure factor $S(\mathbf{q})$ of our colloidal system at three different inverse temperatures corresponding to the isotropic liquid ($\Gamma = 52.4$), the hexatic phase ($\Gamma = 59.6$) and the crystalline ($\Gamma = 61.0$) phase. The central cross is an artifact of the Fourier transformation.

via video-microscopy (resolution of particle position $dr = 100$ nm) and digital image processing over a period of 1–2 h using a frame rate of 250 ms.

To set the stage we first visualize in Fig. (1) the three phases and their symmetries by plotting the structure factor

$$S(\mathbf{q}) = \frac{1}{N} \langle \sum_{i,j} e^{i\mathbf{q}(\mathbf{r}_i - \mathbf{r}_j)} \rangle; \quad (1)$$

as calculated from the positional data of the colloids for three different temperatures. Here, $\langle \cdot \rangle$ runs over all N particles in the field of view while $\langle \cdot \rangle_t$ denote the time average over 700 configurations. In the liquid phase, concentric rings appear having radii that can be connected to typical inter-particle distances. The hexatic phase, on the other hand, is characterized by six segments of a ring which arise due to the quasi-long-range orientational order of the six-fold director [28]. In the crystalline phase the Bragg peaks of a hexagonal crystal show up with a finite width that is due to the quasi-long-range character of the translational order.

To quantify the six-fold orientational symmetry the bond-order correlation function

$$G_6(r) = \langle \cos(6\theta_{ij}(r)) \rangle; \quad (2)$$

is calculated with $\cos(6\theta_{ij}(r)) = \frac{1}{N_j} \sum_j e^{6i\theta_{ij}(r)}$. Here the sum runs over the N_j next neighbors of the particle i at position \mathbf{r} and $\theta_{ij}(r)$ is the angle between a fixed reference axis and the bond of the particle i and its neighbor j . $\langle \cdot \rangle_t$ here denotes not only the ensemble average which is taken over all $N(N-1)/2$ particle-pair distances for each configuration (resolution $dr = 100$ nm) but also the time average over 70 statistically independent configurations.

KTHNY theory predicts that

$$\begin{aligned} \lim_{r \rightarrow \infty} G_6(r) &\neq 0 && \text{crystal: long range order} \\ G_6(r) &\sim r^{-6} && \text{hexatic: quasi long range} \\ G_6(r) &\sim e^{-r/\xi_6} && \text{isotropic: short range}; \end{aligned}$$

$\xi_6 < 1=4$ and takes the value $1=4$ right at $T = T_i$. All three regimes can be easily distinguished in Fig. (2) showing $G_6(r)$ for a few representative temperatures. Note, that $G_6(0)$ is not normalized to 1.

We next fit $G_6(r)$ to r^{-6} and e^{-r/ξ_6} to extract ξ_6 and ν_6 . The fits are performed for radii $r = a \sqrt{20}g$ [29]. To check for the characteristics of the orientational correlation function, the ratio of the reduced chi-square

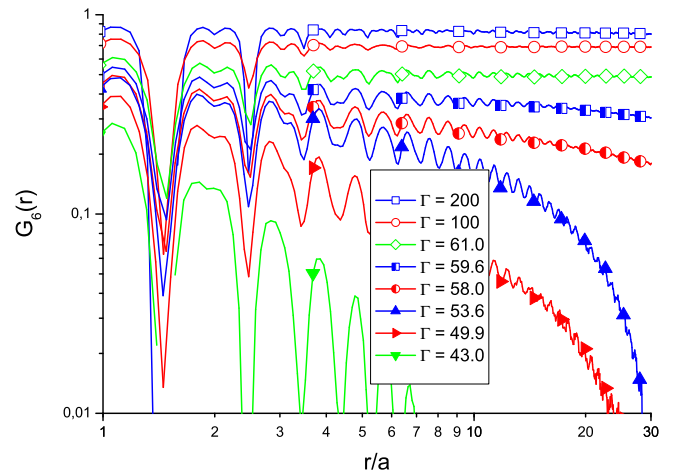


FIG. 2: Orientational correlation function $G_6(r)$ as function of the inverse temperature in a log-log plot. From top to bottom: Three curves for the crystalline phase showing the long-range orientational order ($\lim_{r \rightarrow \infty} G_6(r) \neq 0$), two curves showing the quasi-long-range order of the hexatic phase ($G_6(r) \sim r^{-6}$) and three curves showing the short-range order typical of the isotropic liquid ($G_6(r) \sim e^{-r/\xi_6}$).

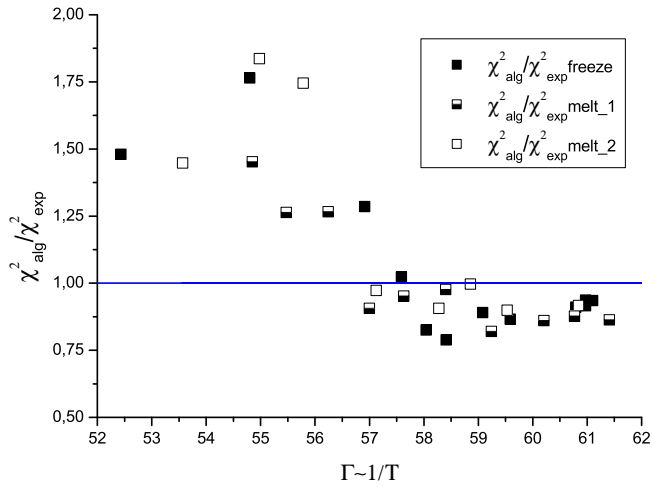


FIG. 3: Quantitative test for the long distance behavior of $G_6(r)$. For $\chi^2_{alg} = \chi^2_{exp} < 1$ the algebraic decay fits better.

χ^2 goodness-of-fit statistic of the algebraic (χ^2_{alg}) and exponential (χ^2_{exp}) fits is shown in Fig. (3) as a function of Γ for three different measurements. For melting, a crystal free of dislocations was grown at high Γ and then Γ was reduced in small steps. For each temperature step the system was equilibrated 1=2 h before data acquisition started. This was done at different densities: melt_1 with average particle distance of $a = 11.8$ nm and melt_2 with $a = 14.8$ nm containing 3200 respectively 2000 particles in the field of view. The measurement denoted freeze in Fig. (3) ($a = 11.8$ nm) started in the isotropic liquid phase and Γ was increased with an equilibration time of 1 h between the steps. For $\chi^2_{alg} = \chi^2_{exp} > 1$ an exponential decay fits better than the algebraic and vice versa for $\chi^2_{alg} = \chi^2_{exp} < 1$. We observe in Fig. (3) that the change in the characteristic appears at $\Gamma_i = 57.5 \pm 0.5$. This value is the temperature of the hexatic \leftrightarrow isotropic liquid transition.

In the vicinity of the phase transition, approaching Γ_i from the isotropic liquid the orientational correlation length ξ_6 should diverge as [4],

$$\xi_6(\Gamma) \sim \exp\left(\frac{b}{\Gamma - \Gamma_i}\right); \quad (3)$$

with b a constant and $\Gamma = 1=2$. This behavior is observed in Fig. (4a). ξ_6 indeed increases dramatically near $\Gamma_i = 57.5 \pm 0.5$ irrespective of whether the system is heated or cooled. Before discussing this feature we first address the finite size effect. To this end, we have computed $G_6(r)$ and ξ_6 for subsystems of different size ranging from 720×515 nm²; 615×405 nm²; 505×300 nm²; 400×190 nm² to 390×80 nm². The resulting data-points are plotted as triangles in Fig. (4) and belong to the black filled squares which they converge to. No finite size effect is found for $\Gamma < 56$, but a considerable one at $\Gamma = 56.9$ close to Γ_i where we obviously need the full field of view to capture

the characteristic of the divergence. At $\Gamma = 58.0$ there is a huge finite size effect indicating that ξ_6 is much larger than the field of view. However, inside the hexatic phase, ξ_6 is no longer well defined as the decay is algebraic. We fit our data to eq. (3) in the range $49 < \Gamma < 57.5$ and find the critical exponent $\nu = 0.5 \pm 0.03$ and $\Gamma_i = 58.9 \pm 1.1$, a value which due to the finite-size effect is slightly larger than Γ_i obtained from Fig. (3).

The exponent ν is related to Frank's constant F_A [4]

$$\nu = \frac{18k_B T}{F_A(\Gamma)}; \quad (4)$$

So the critical exponent $\nu(\Gamma_i) = 1=4$ corresponds to $F_A(\Gamma_i) = 72=$ at the hexatic \leftrightarrow liquid transition. This quantity is plotted in Fig. (4b). Indeed, F_A crosses the value $72=$ at $\Gamma_i = 57.5 \pm 0.5$ exactly at that temperature which in Fig. (3) has been independently determined to

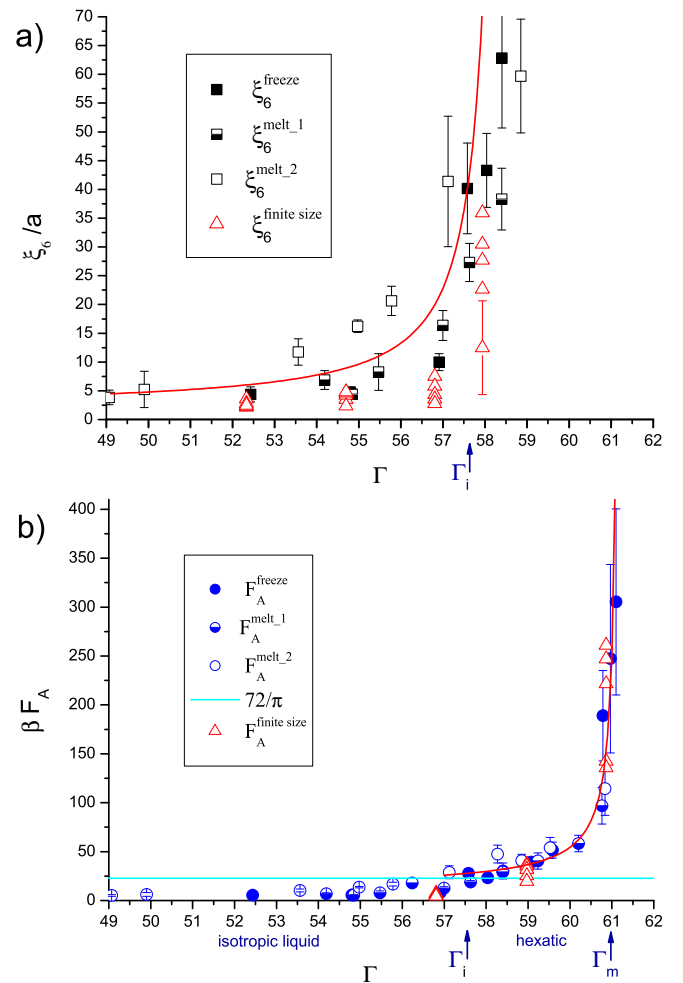


FIG. 4: Correlation length ξ_6 (a) and Frank constant F_A (b) as a function of the inverse temperature. ξ_6 diverges at Γ_i and F_A at Γ_m . In between the system shows hexatic symmetry. The solid lines are fits to eq. (3) and (5) resulting in critical exponents $\nu = 0.5 \pm 0.03$ and $\nu = 0.35 \pm 0.02$ respectively. Triangles are shifted by 0.1 for clarity.

be the transition temperature T_i . For $T < T_i$, F_A should jump to zero which is not completely reproduced. We note that since ξ is not well defined in the isotropic fluid, it becomes problematic to extract F_A from eqn. (4) below T_i . At T_m , at the hexatic \rightarrow crystalline transition, F_A must diverge which indeed it does. This divergence can be identified with the divergence of the square of the translational correlation length ξ^2 [4]

$$F_A(T) = k_B T \sum_{j=1}^2 \exp\left(-\frac{2c}{1 - \xi_j^2}\right); \quad (5)$$

where c is again a constant and $\xi = 0.36963$. Fitting the values of F_A to the expression in eqn. (5) in the range $57.5 < T < 61$ we obtain $\xi = 0.35 \pm 0.02$ and $T_m = 61.3 \pm 0.4$ as an upper threshold. A gain triangles represent evaluation of our data in sub-windows of variable size (same sizes as above). The finite size effect for $T = 57.0$ is negligible. Close to T_m it increases but the values saturates for $T = 59.1$ and $T = 60.8$ and remain within the error-bars for the biggest sub-windows.

In conclusion, we have checked quantitatively the change of quasi-long-range to short-range orientational order and extracted the correlation length ξ in the isotropic fluid and Frank's constant F_A in the hexatic phase from trajectories of a 2d colloidal system. We find a hexatic \rightarrow isotropic liquid transition at $T_i = 57.5 \pm 0.5$. Three observations support this result: (i) the change of the distance dependence of $G_\xi(r)$ (Fig. (3)), (ii) the condition $F_A(T_i) = 72=$ for Frank's constant and (iii) the divergence of ξ . For the transition hexatic \rightarrow crystal F_A diverges at T_m . Both divergencies (extracted from just one correlation function) lead to critical exponents that are in good agreement with the KTHNY-theory. The measurements for melting and freezing support each other; so we may conclude that there is no hysteresis effect of the phase-transitions. At the two transitions, the order parameters are observed to change continuously (within the resolution of $\Delta T = 1$); no indication of a phase-separation (as for example strong fluctuations of the order parameters) has been found [30] as has been reported by [17, 21]. So we believe that in our system – having a well-defined, purely repulsive pair-potential and a conformation to 2D that is free of any surface roughness – the transitions are second order.

In [31, 32] we verified that the Young's modulus becomes 16 at T_m . We have now checked that F_A takes the value $72=$ at T_i . These two findings together confirm the two-stage KTHNY melting scenario with its underlying microscopic picture of breaking the translational symmetry by dislocation-pair- and orientational symmetry by disclination-pair-unbinding.

P. Keim gratefully acknowledges the financial support of the Deutsche Forschungsgemeinschaft.

-
- [1] J. Kosterlitz and D. Thouless, *J. Phys. C*, **6**, 1181 (1973).
 - [2] A. P. Young, *Phys. Rev. B*, **19**, 1855 (1979).
 - [3] B. I. Halperin and D. R. Nelson, *Phys. Rev. Lett.* **41**, 121 (1978).
 - [4] D. R. Nelson and B. I. Halperin, *Phys. Rev. B* **19**, 2457 (1979).
 - [5] S. T. Chui, *Phys. Rev. B* **28**, 178 (1983).
 - [6] H. Kleinert, *Phys. Lett.* **95A**, 381n (1983).
 - [7] M. A. G. Lasler and N. A. Clark, *Adv. Chem. Phys.* **83**, 543 (1993).
 - [8] Y. Lansac, M. A. G. Lasler, and N. A. Clark, *Phys. Rev. E* **73**, 041501 (2006).
 - [9] K. Chen, T. Kapan, and M. M. Ostoller, *Phys. Rev. Lett.* **74**, 4019 (1995).
 - [10] F. L. Sommer, G. S. Canright, T. Kapan, K. Chen, and M. M. Ostoller, *Phys. Rev. Lett.* **79**, 3431 (1997).
 - [11] C. H. Mak, *Phys. Rev. E*, **73**, 065104(R) (2006).
 - [12] A. Jaster, *Phys. Rev. E* **59**, 2594 (1999).
 - [13] S. Z. Lin, B. Zheng, and S. Trimper, *Phys. Rev. E*, **73**, 066106 (2006).
 - [14] C. A. Murray and D. H. Van Winkle, *Phys. Rev. Lett.* **58**, 1200 (1987).
 - [15] Y. Tang, A. J. Armstrong, R. C. Mockett, and W. J. O'Sullivan, *Phys. Rev. Lett.* **62**, 2401 (1989).
 - [16] R. E. Kusner, J. A. Mann, J. Kerins, and A. J. Dahm, *Phys. Rev. Lett.* **73**, 3113 (1994).
 - [17] A. H. Marcus and S. A. Rice, *Phys. Rev. Lett.* **77**, 2577 (1996).
 - [18] K. Zahn and G. Maret, *Phys. Rev. Lett.* **85**, 3656 (2000).
 - [19] A. V. Petukhov, D. van der Beek, R. P. A. Dullens, I. P. Dolbnya, G. J. Vroege, and H. N. W. Lekkerkerker, *Phys. Rev. Lett.* **95**, 077801 (2005).
 - [20] R. A. Segalman, A. Hexemer, R. C. Hayward, and E. J. Kramer, *Macromolecules*, **36**, 3272 (2003).
 - [21] D. E. Angelescu, C. K. Harrison, M. L. Trawick, R. A. Register, P. M. Chaikin, *Phys. Rev. Lett.* **95**, 025702 (2005).
 - [22] R. Seshadri and R. M. Westervelt, *Phys. Rev. B*, **46**, 5142 (1992).
 - [23] P. M. Reis, R. A. Ingale, and M. D. Shattuck, *Phys. Rev. Lett.* **96**, 258001 (2006).
 - [24] X. H. Zheng and R. Grieve, *Phys. Rev. B*, **73**, 064205 (2006).
 - [25] P. Dimon, P. M. Hom, M. Sutton, R. J. Birgeneau, and D. E. Moncton, *Phys. Rev. B*, **31**, 437 (1985).
 - [26] D. Li and S. A. Rice, *Phys. Rev. E*, **72**, 041506 (2005).
 - [27] P. Keim, G. Maret, U. Herz, and H. H. von Grunberg, *Phys. Rev. Lett.* **92**, 215504 (2004).
 - [28] The segments will merge to rings, if the system size tends towards infinity.
 - [29] The upper value is motivated by the maximum value of the histogram of distances and $r=a=0$ is excluded in the algebraic case to avoid the singularity. The histogram over distances is used as statistical weight of the t -function taking into account the different frequency of occurrence of the data-points in the minimum and maximum of $G_\xi(r)$.
 - [30] We indeed do see a local clustering of dislocations as already noted by [14, 15] in the hexatic phase close to T_i (which is not too surprising for dislocations with finite density having an attractive interaction) but this averages out in G_ξ if the field of view is big enough.

- [31] H. H. von Grunberg, P. Keim, K. Zahn, and G. Maret, Phys. Rev. Lett. 93, 255703 (2004).
Cond. Mat. 17, 3579 (2005).
- [32] J. Zanghellini, P. Keim, and H. H. von Grunberg, J. Phys.